

Fine structure of Rydberg states. II. $n = 8$ and 9 D and F states and $n = 16, 17,$ and 18 P and D states of ${}^4\text{He}^\dagger$

Keith B. MacAdam

Department of Physics, University of Arizona, Tucson, Arizona 85721

William H. Wing

Department of Physics and Optical Sciences Center, University of Arizona, Tucson, Arizona 85721

(Received 26 January 1976)

We report high-precision measurements of fine-structure intervals in Rydberg states of ${}^4\text{He}$ as follows: 8^1D_2 - $8^{1,3}F_3$ and $9^3D_{2,3}$ - $9^{1,3}F_3$ near 21 GHz and n^1P_1 - n^1D_2 for $n = 16, 17,$ and 18 near 23, 19, and 16 GHz, respectively. A microwave-optical-resonance method and electron-bombardment excitation were used. We state and discuss formulas for predicting as yet unobserved members of n^1D_2 - $n^{1,3}F_3$ and n^1P_1 - n^1D_2 series. We give an accurate result for the 9^1D_2 - 9^3D_2 interval obtained indirectly from our work. New results on singlet-triplet mixing coefficients in F states and on coefficients in a Ritz series expansion of quantum defects are also given.

I. INTRODUCTION

In several publications¹⁻⁵ from our laboratories we have reported microwave resonances in Rydberg states of helium. The work has primarily involved transitions from D to F states, and in addition a few preliminary results were given^{3,4} involving transitions to G and H states ($L = 4$ and 5). The principal quantum number, which does not change in the transitions observed, has ranged from $n = 6$ to $n = 11$.

In the work reported here, we used the same method to observe transitions as follows: 8^1D_2 - $8^{1,3}F_3$ and $9^3D_{2,3}$ - $9^{1,3}F_3$ near 21 GHz, 16^1P_1 - 16^1D_2 near 23 GHz, 17^1P_1 - 17^1D_2 near 19 GHz, and 18^1P_1 - 18^1D_2 near 16 GHz. The resonances in $n = 8$ and 9 give us further information on the D and F series of levels, while the $n = 16$ - 18 resonances represent a series not previously observed in these experiments. The only other transition frequency measured directly in an nP - nD series is the interval 3^1P_1 - 3^1D_2 measured by Levine, Sanchez, and Javan⁶ by frequency-mixing methods using the 93.5 - μm output of a pure helium laser.

Several other groups, both theoretical and experimental, have obtained results recently on highly-excited states in helium. Chang and Poe^{7,8} have calculated electrostatic and relativistic fine structure in highly excited D , F , and G states using Brueckner-Goldstone perturbation theory. Their results are the best available, but nonetheless they lie outside the error bars of the present work. Van den Eynde *et al.*⁹ and Parish and Mires¹⁰ have calculated energy levels and singlet-triplet mixing coefficients in Rydberg states of helium, but the shortcomings of these calculations have been previously mentioned by others and by ourselves.^{5,7,8}

Miller *et al.*,¹¹ Derouard *et al.*,¹² and Beyer and Kollath¹³ have recently measured n^1D - n^3D splittings in highly excited states of helium using anti-crossing methods from $n = 3$ to 11 . Similar preliminary measurements have been made by Beyer and Kollath¹⁴ as far as $n = 20$. Through an indirect result of our work we can state a value for the 1D_2 - 3D_2 splitting in $n = 9$ that has an uncertainty an order of magnitude smaller than the result of Beyer and Kollath (Sec. IV A).

The apparatus and method will be described briefly in Sec. II. The new results will be given in Sec. III and discussed in Sec. IV.

II. EXPERIMENTAL METHOD AND APPARATUS

The experimental method was described in detail in Ref. 5 (hereafter referred to as I). In brief, helium at pressures of approximately 10^{-3} Torr is continuously excited to the states of interest by electron bombardment in a section of waveguide free of static fields. Fluorescence of the excited atoms is monitored by a small monochromator and photomultiplier. When microwave (rf) power is introduced into the waveguide at a frequency corresponding to an electric dipole transition, a small change is noted in the fluorescence intensity from either of the levels connected by the transition. This change is measured with a lock-in amplifier to detect the resonance.

The microwave apparatus was that described in I with minor changes. An X -band Hewlett-Packard H01-694A sweep oscillator was phase locked to a low-frequency synthesizer. The sweep oscillator output was amplified by an Alfred 528A TWT amplifier, and the rf power was chopped and leveled by a Hewlett-Packard 8734B PIN modulator. The rf was frequency doubled by a 1N53B diode placed

across a short section of waveguide, and the fundamental power was removed by using a waveguide section below cutoff.

The line-shape formula is given in I, where it is shown that the linewidth in the limit of zero rf perturbation is the sum of the natural widths of the two states in resonance. The line shape is Lorentzian in the same limit. At higher values of rf intensity a Lorentzian function still fits the data adequately, although the actual profile is a sum of several Lorentzians of differing heights and widths that have a common center. These arise from the degenerate M_J sublevels of the resonating states.

For sufficiently long-lived states the line shape will be modified by the thermal displacement of the atoms during their decay. A highly excited atom may move during its life from a node to an antinode of the rf standing-wave pattern in the waveguide, its image at the photomultiplier may sweep over areas of varying photocathode sensitivity, or it may even pass out of the field of view entirely while decaying. Thus the probability amplitude for detection of its decay light as a function of time after excitation will vary in a non-exponential manner. These effects, averaged over the excitation volume, would be unlikely to shift the line center but would prevent a simple interpretation of the linewidth.¹⁵

In the case of $n = 18$, the 1P lifetime is $0.35 \mu\text{sec}$

and that of 1D is $3.4 \mu\text{sec}$.¹⁶ At high rf power levels, such as were used here, the atom decays in a mean time approximately equal to twice the 18^1P lifetime.¹⁷ At a velocity of 10^5 cm/sec a typical thermal displacement is therefore 0.07 cm . This is smaller than both the 16-GHz rf wavelength ($\lambda/2\pi = 0.30 \text{ cm}$) and the dimensions of the waveguide ($\approx 1 \text{ cm}$). Thus in the present case the effects of atomic thermal motion on the line shape should be small. However, in the case of the longer-lived triplet states, or of states with higher principal quantum numbers, the effects will be substantially larger and will complicate a detailed line-shape analysis.

III. RESULTS

A. $n=8$ resonances

The $8^1D_2-8^1F_3$ resonance at $21\,226 \text{ MHz}$ was scanned 42 times using various pressures, bombarding voltages and currents, and rf power levels. The fitted centers ranged from $21\,225.59$ to $21\,226.54 \text{ MHz}$ and showed a tendency toward the lower values in later runs. It became clear that charging of the interior of the waveguide near the electron beam was responsible for Stark shifts to lower frequencies. Therefore greater weight was placed on the earlier values obtained. The center frequency and standard deviation quoted in Table I

TABLE I. Summary of new results in ^4He .

Transition	Frequency ^a (MHz)	Other results ^b (MHz)
$8^1D_2-8^1F_3$	$21\,226.4 \pm 0.2$	$20\,886^c$ (T)
$8^1D_2-8^3F_3$	$21\,126.5 \pm 0.2$	$20\,789^c$ (T)
$9^3D_2-9^1F_3$	$21\,607.2 \pm 0.1$	$21\,322^c$ (T)
$9^3D_3-9^1F_3$	$21\,610.7 \pm 0.3$	$21\,325^{c,d}$ (T)
$9^3D_2-9^3F_3$	$21\,536.2 \pm 0.3$	$21\,253^c$ (T)
$9^3D_3-9^3F_3$	$21\,540.2 \pm 0.5$	$21\,256^{c,d}$ (T)
$16^1P_1-16^1D_2$	$22\,807.5 \pm 0.3^e$	$22\,750^f$ (E)
$17^1P_1-17^1D_2$	$19\,021.5 \pm 0.4^e$	$18\,970^f$ (E)
$18^1P_1-18^1D_2$	$16\,029.4 \pm 0.6^e$	$15\,990^f$ (E)
Derived interval	Frequency (MHz)	Other results (MHz)
$8^1F_3-8^3F_3$	99.9 ± 0.3	97.3^c (T)
$9^1F_3-9^3F_3$	71.1 ± 0.3	69.1^c (T)
$9^3D_2-9^3D_3$	3.5 ± 0.4	2.9^d (T)
$9^1D_2-9^3D_2$	6658.8 ± 0.6^g	6652 ± 35^h (E)

^a Present work. Uncertainties are one standard deviation.

^b T, theoretical; E, experimental.

^c Chang and Poe, Ref. 7.

^d Chang and Poe, Ref. 8.

^e Stark corrections have been applied as described in Sec. IV A.

^f Seaton, quantum-defect fit of experimental data, Ref. 18.

^g Present work, using $9^3D_2-9^1F_3$ measurement and $n^1D_2-n^1F_3$ series formula for $n=9$. See Sec. IV A.

^h Based on Beyer and Kollath, Ref. 13. See text, Sec. IV A.

make appropriate allowance for the Stark shifts as well as for the purely statistical variation of the line centers. The linewidths varied from 1.5 to 3.0 MHz, depending on the values of rf power used. Observation time for a given resonance scan was about 35 min and the signal-to-noise ratio varied from 10 to 50 at the line centers.

The $8^1D_2-8^3F_3$ resonance at 21 126 MHz was scanned eleven times. It also showed a gradually increasing Stark shift in the later runs. In other respects this transition was similar to $8^1D_2-8^1F_3$. The line-center result is listed in Table I. For both $n=8$ resonances the fluorescence of the 8^1D state was monitored at 3926.5 Å.

B. $n=9$ resonances

There are eight allowed electric dipole transitions from the fine-structure levels of the 9^3D term to the $9F$ term. The corresponding set of eight resonances in $n=7$ was reported in I. However, in the present work, because of poorer signal-to-noise ratios and the charging effect noted in Sec. IIIA, only the four resonances $9^3D_{2,3}-9^1F_3$ and $9^3D_{2,3}-9^3F_3$ could be accurately measured. The splitting between the 9^3D_2 and 9^3D_3 levels is only about 3.5 MHz, so the four resonances appeared as two partially resolved pairs. The $9^3D_2-9^1F_3$ peaks were four times as high as the $9^3D_3-9^1F_3$ peaks, and the linewidths were about 2 MHz [Fig. 1(a)]. The resonances were detected by monitoring the 9^3D -state fluorescence at 3587 Å. The $n=9$ resonances were observed under conditions of relatively high helium pressure, that is, high enough that the population of $9F$ states produced by collisional excitation transfer from 9^1P states exceeded the population of 9^3D states produced directly by electron impact or indirectly by cascades or collisional transfer. Correspondingly, the resonances appeared with a polarity the reverse of that observed for the 8^1D-8F resonances. The same effect was noted in I in a comparison of 7^3D-7F and 6^1D-6F resonances. The results for the $n=9$ resonances are given in Table I.

C. $n=16, 17,$ and 18 resonances

The $n^1P_1-n^1D_2$ resonances presented a search problem, since no accurate measurements in this series above $n=3$ had been made. Since the quantum-defect fit of optical spectroscopic data performed by Seaton¹⁸ tends to smooth the random variations in the data, we felt that it would give useful estimates of the resonance frequencies for $n=16-18$. This proved to be the case, and the resonances were each found about 60 MHz higher than the predicted line center, a remarkable suc-

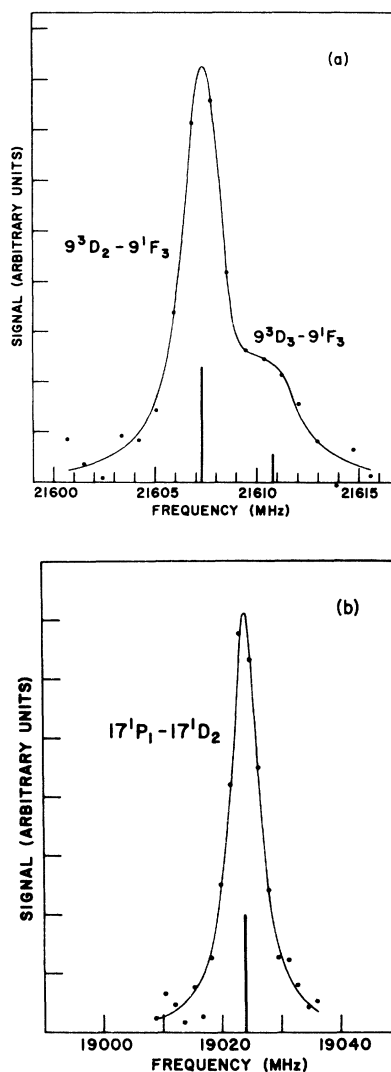


FIG. 1. Resonance curves. (a) $9^3D_2-9^1F_3$ and $9^3D_3-9^1F_3$. The radiative widths of these resonances are about 0.7 MHz. (b) $17^1P_1-17^1D_2$. The radiative width is about 0.6 MHz. The dots are results of 100-sec integrations of the lock-in amplifier output. The curves are computer fits to the data, assuming Lorentzian line shapes. The vertical bars are placed at the fitted line centers.

cess in view of the typical 0.01-cm^{-1} (300 MHz) accuracy of the optical data. Several scans of the $n=16$ and 17 resonances were made, but only two successful scans of the $n=18$ resonance were obtained because of its significantly poorer signal-to-noise ratio. The linewidths in each case were about 6 MHz, an order of magnitude greater than the minimum width set by the radiative lifetimes of the states [Fig. 1(b)]. We attribute this excess width to rf power broadening and Stark broaden-

TABLE II. Constants for the fitting formula Eq. (1). See Figs. 2–5 for estimated error bands of transition frequencies predicted from these values. The parameters A , B , and C predict the intervals for zero electrostatic field.

Transition	Data used	A (GHz)	B (GHz)	C (GHz)
$n {}^1D_2-n {}^1F_3$	$n=6-8, 10, 11$	11 008.3	-8 950	-2 800
$n {}^1D_2-n {}^3F_3$	$n=6-8, 10, 11$	10 953.1	-8 640	-5 900
$n {}^1F_3-n {}^3F_3$	$n=6-11$	55.15	-304	2 900
$n {}^1P_1-n {}^1D_2$	$n=3-10, 16-18$ ^a	93 712.8	-74 800	-72 800

^a Separate Stark corrections were applied for $n=6-10$ and for $n=16-18$.

ing. Relatively high rf fields were required because small random electrostatic fields spread the line centers for atoms in different parts of the waveguide over as much as 2 or 3 MHz. By power broadening the resonances to about 6 MHz most atoms could be made to contribute at once to the resonance, which consequently brought the height at the line center well above the noise level. Slight asymmetries of the lines were noted, as would be expected from a quadratic Stark effect, and the electrostatic fields shifted the lines slightly to higher frequencies. This direction of shift is opposite to that for the D -to- F resonances because $n {}^1P$ terms lie above all other nL terms. The $n=16$ resonance was detected using both $16 {}^1P-2 {}^1S$ (3163 Å) and $16 {}^1D-2 {}^1P$ (3738 Å) fluorescence lines, and it appeared with opposite polarity in the two cases as expected. The $n=17$ and 18 resonances were monitored using only fluorescence from the D state because of the higher quantum efficiency of the photomultiplier at the longer wavelengths.

Although we were unable to control or to measure the small electrostatic fields that gave rise to the Stark shifts, we were able to estimate line-center corrections by using a fitting formula such as Eq. (1) below. The corrected line centers are given in Table I for the $n=16-18 {}^1P_1-{}^1D_2$ resonances. The Stark corrections are discussed in Sec. IV A.

IV. DISCUSSION

A. Series formulas

On the basis of the present measurements the "fitting formulas" given in I for $n {}^1D_2-n {}^1F_3$ splittings can be improved and new formulas given. The expression

$$\nu_n = A/n^3 + B/n^5 + C/n^7 \quad (1)$$

was fitted to the data for transitions in a given series by a weighted linear least-squares routine.¹⁹ The resulting coefficients A , B , and C and their estimated standard deviations have proven useful in predicting frequencies for series mem-

bers not yet measured. For instance, using the coefficients given in Table VI of I, the $n=8$ resonances reported here were predicted within 1.5 MHz.

The $n=8$ measurements were combined with $n=6, 7, 10$, and 11 results from previous work,³⁻⁵ and new coefficients were obtained as listed in Table II. From the predicted frequency of the $9 {}^1D_2-9 {}^1F_3$ transition, $14\,948.4 \pm 0.6$ MHz, and the frequency of the $9 {}^3D_2-9 {}^1F_3$ transition reported in Table I, we can deduce the value 6658.8 ± 0.6 MHz for the $9 {}^1D_2-9 {}^3D_2$ splitting (68% confidence level). Beyer and Kollath¹³ have reported a value for the $9 {}^1D_2-9 {}^3D_{\text{mean}}$ interval. For comparison with our work we add to their value the $9 {}^3D_{\text{mean}}-9 {}^3D_2$ interval obtained by scaling our data in I by $1/n^3$. The result is 6652 ± 35 MHz. Their uncertainty represents a 95% level of confidence.¹⁴ Therefore, based on the proven reliability of the fitting formulas and on our $9 {}^3D-9F$ measurements, we have an indirect result with an uncertainty many times smaller than previously obtained by a more direct method.

The least-squares routine used to fit Eq. (1) to the data provides the complete variance-covariance matrix for the parameters.²⁰ From this the parameter errors can be propagated back to the predicted frequencies for any value of n . We can estimate the standard deviations of the predictions of series members not necessarily observed by using the variance-covariance matrix of the predictions,

$$M_\nu = T M_A T' \quad (2)$$

The variance-covariance matrices of parameters and predictions are M_A and M_ν , respectively. T is a rectangular matrix whose rows are the derivatives of Eq. (1) with respect to each parameter in turn, evaluated at the quantum number n . T' is its transpose. Estimates of the standard deviations of the predictions, i.e., the error bands, are given by the square roots of the diagonal elements of M_ν . Figures 2 and 3 show error bands calculated in this way for the $n {}^1D_2-n {}^1F_3$ and $n {}^1D_2-n {}^3F_3$ series. The figures show that

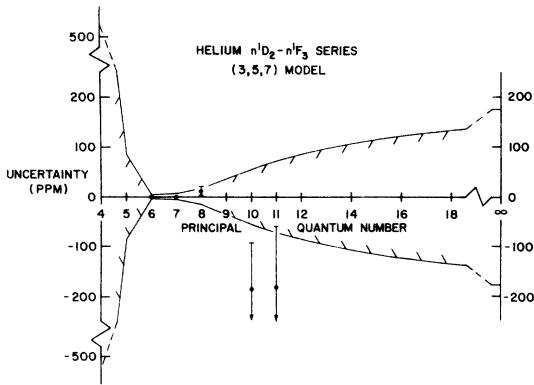


FIG. 2. Error bands for predictions of $n^1D_2 - n^1F_3$ intervals in helium (see text, Sec. IV A). The data points shown represent the relative discrepancies between our measurements (Table I and Refs. 3–5) and the predicted frequencies (Table II). The arrows indicate that the $n=10$ and 11 error bars lie off-scale in the directions indicated. The typical discrepancy between data and prediction is of the same order as the SD of the datum, a result to be expected in the weighted least-squares fit used to obtain the predictions. The error bands and predictions for the $D-F$ and ${}^1F_3 - {}^3F_3$ sequences are significantly model dependent for $n < 6$.

where accurate measurements are available, predictions can be made with corresponding accuracy, as is intuitively clear. In fact the standard deviations (SD's) of the predictions are often smaller than the SD's of the original measurements, since *all* the measurements contribute to the knowledge of the frequency at a given n , assuming that Eq. (1) is a correct model. In the error-band figures, 56% of the data points lie within the error bands and 59% of the (1-SD) error bars of the data overlap the corresponding predictions. In the absence of systematic or model errors these values would

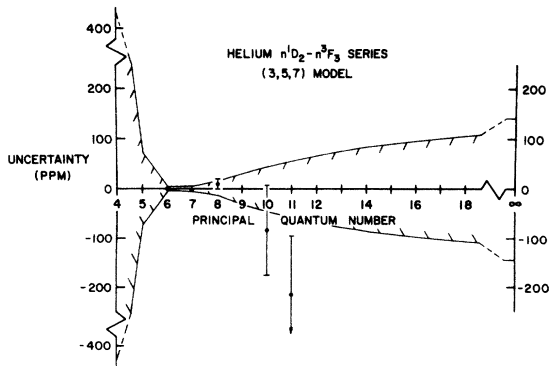


FIG. 3. Error bands for predictions of $n^1D_2 - n^3F_3$ intervals in helium. See caption to Fig. 2.

be expected to approximate 68%. Outside the range of n 's measured, the uncertainty of the fit increases, illustrating the principle that one should be wary of extrapolations. The (relative) uncertainty becomes asymptotically constant in the limit of high n , reflecting the fact that in this limit only the first term of Eq. (1) contributes. Owing to the very high correlation of the parameter errors that results from the nonorthogonal basis functions used in Eq. (1), prediction errors for nearby values of n are also strongly correlated.

From the measurements reported above, we can extract values for the $n^1F_3 - n^3F_3$ splitting in $n=8$ and 9 (see Table I). Including previous results,³⁻⁵ we now have accurate values for this splitting for $n=6-11$ inclusive. The coefficients A , B , and C in Eq. (1) are given in Table II for this series. Figure 4 shows error bands for the $n^1F_3 - n^3F_3$ predictions.

A fitting formula can also be constructed for the series $n^1P_1 - n^1D_2$ from the present results. Levine, Sanchez, and Javan⁶ have obtained 3129791.5 ± 3.0 MHz for the $n=3$ interval. Intervals for the $n=4-10$ can be extracted from Martin's compilation²¹ of helium spectral data at a much lower level of accuracy. It appears from fitting Eq. (1) to the available data for $n=3-10$ and $16-18$ that the intervals for $n=6-10$ from Martin's table have a scatter several times as large as indicated by the number of significant figures given. The tabulated energy levels are given to 0.01 cm^{-1} , whereas the typical deviation from fit is 0.07 cm^{-1} . According to Martin's earlier compilation,²² the energy levels for $n=4$ and 5 derive from more reliable sources than those for $n=6-10$.

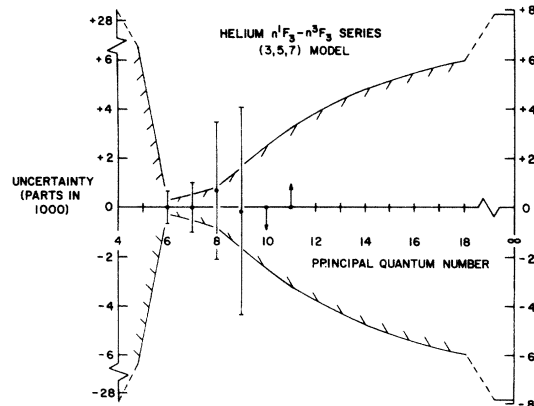


FIG. 4. Error bands for predictions of $n^1F_3 - n^3F_3$ splittings in helium. The dots at $n=10$ and 11 indicate that the data points and their error bars both lie off-scale in the directions indicated by the arrows. See caption to Fig. 2.

We find that the deviations of the intervals $n = 6-10$ taken as a group are consistent with Stark shifts $(1.90 \pm 1.20) \times 10^{-4} n^7$ MHz as would be produced in an electric field on the order of 100 V/cm. This value must be regarded as only typical, since the individual lines contributing to the $n = 6-10$ data were measured at different times by different researchers. However, the electric field is similar to those found in spectroscopic discharge sources.

The deviations of our $n = 16-18$ data also showed a trend that could be explained in terms of Stark shifts. By introducing an additional term proportional to n^7 in Eq. (1), we found Stark-like contributions $(5.0 \pm 0.7) \times 10^{-9} n^7$ MHz for these resonances as would be produced by an electric field in the experimental module on the order of 0.5 V/cm. We subtracted these estimated Stark shifts from our $n = 16, 17,$ and 18 data (1.34, 2.05, and 3.06 MHz, respectively) to obtain the corrected line centers given in Table I. The uncertainties of these Stark corrections and the statistical uncertainties of the line centers are combined in quadrature to give the uncertainties (SD's) in the table.

The Stark corrections were applied separately for $n = 6-10$ and $n = 16-18$, and parameters $A, B,$ and C in Eq. (1) were obtained for the $n^1P_1-n^1D_2$ series. The parameters are listed in Table II. Figure 5 shows error bands for this series. The fitted parameters were not significantly affected if the $n = 6-10$ data were omitted. However, they were substantially altered if the $n = 4$ and 5 data were also left out.

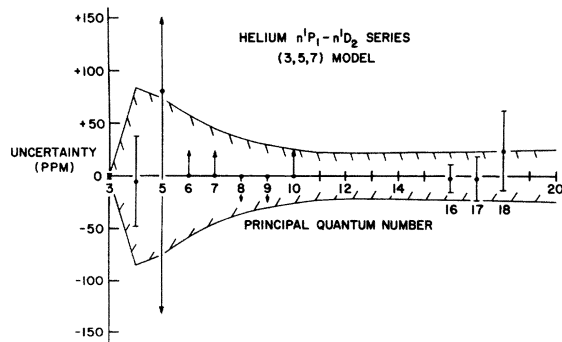


FIG. 5. Error bands for predictions of $n^1P_1-n^1D_2$ intervals in helium. The Stark corrections for $n = 6-10$ and $n = 16-18$ data discussed in Sec. IV A were applied before the prediction uncertainties were calculated. The dots at $n = 6-10$ indicate that the corresponding data and error bars lie off-scale in the direction of the arrows.

B. Quantum defects

The coefficients $A, B,$ and C in Eq. (1) can be related to quantum-defect differences. If a Ritz series expansion for the quantum defects in helium exists, namely,

$$\mu_n = C_2 + C_3 \epsilon + C_4 \epsilon^2 + \dots, \quad (5)$$

where μ_n is the quantum defect for principal quantum number n and $\epsilon = -(n - \mu_n)^{-2}$ is the binding energy in rydbergs,¹⁸ then in general an expansion of a series of transition frequencies contains all integral inverse powers of n greater than 2. However, it appears in practice that the inverse even powers are less significant than the odd powers (see the Appendix). In fact Chang²³ has shown that in a certain approximation the expansion contains only inverse *odd* powers. If $A^{(m)}$ denotes the coefficient of the $1/n^m$ term in an expansion such as Eq. (1), then the expansion can be related to Ritz series for the two types of terms as follows:

$$A^{(3)} \equiv A = 2(C_2 - C'_2)Rc, \quad (4)$$

$$A^{(4)} = 3(C_2^2 - C_2'^2)Rc, \quad (5)$$

$$A^{(5)} \equiv B = [4(C_2^3 - C_2'^3) - 2(C_3 - C_3')]Rc, \quad (6)$$

etc. The primed Ritz-series coefficients are those for the higher-lying state. R is the Rydberg constant for helium (cm^{-1}) and c is the speed of light.

Using an incomplete set of imperfect data, the values of coefficients $A^{(m)}$ obtained in a least-squares fit depend on which powers m are included in the model. Our experience with the available data is that of all three-parameter models the (3, 5, 7) model, Eq. (1), fits better than any other choice of exponents. The quality of the data from our work and that of others is in no case good enough to give meaningful fits with four or more such parameters.

Seaton's values¹⁸ of the Ritz-series coefficients can be used as a first approximation to show that in Eq. (6) the first term $4(C_2^3 - C_2'^3)$ is negligible compared with the second term. Therefore from the (3, 5, 7) fits of Table II we can obtain the Ritz-coefficient differences ΔC_2 and ΔC_3 shown in Table III.

C. Relativistic fine structure

The relativistic fine-structure interval $9^3D_2-9^3D_3$ is seen from Table I to be 3.5 ± 0.4 MHz. The 10% SD of this small splitting is so large that we can conclude only that it is consistent with the value $(\frac{7}{3})^3 \times 7.1 = 3.3$ MHz scaled from our result in $n = 7$.⁵

TABLE III. Ritz-coefficient differences from (3, 5, 7) fits in Table II using Eqs. (4) and (6). Here, $\Delta C_i = C_i - C'_i$. ΔC_2 is the constant part of the difference of quantum defects for the two states connected by the transition. ΔC_3 is the part of the difference linear in binding energy.

Transition	$\Delta C_2^{\text{expt } a}$	$\Delta C_2^{\text{Seaton } b}$	$\Delta C_3^{\text{expt } a}$	$\Delta C_3^{\text{Seaton } b}$
$n \ ^1D_2 - n \ ^1F_3$	1.6733 (3) $\times 10^{-3}$		1.36 (3) $\times 10^{-3}$	
$n \ ^1D_2 - n \ ^3F_3$	1.6649 (2) $\times 10^{-3}$		1.31 (2) $\times 10^{-3}$	
$n \ ^1P_1 - n \ ^1D_2$	1.424 47(3) $\times 10^{-2}$	1.4217 $\times 10^{-2}$	1.137(5) $\times 10^{-2}$	1.009 $\times 10^{-2}$

^a Present work. The uncertainties quoted are statistical only. See the Appendix for a discussion of model-dependent errors.

^b Ritz coefficients from Seaton, Ref. 18. No results are available for 1F_3 and 3F_3 because of the lack of optical spectroscopic data in which the F -state fine structure is resolved.

D. Singlet-triplet mixing coefficients

In I it was shown that singlet-triplet mixing coefficients Ω could be calculated in a semiempirical way from our data. The $n \ ^1F_3 - n \ ^3F_3$ splittings for $n=8$ and 9, together with values of the off-diagonal matrix element of the spin-orbit interaction in the Breit-Bethe approximation, yield mixing coefficients

$$\Omega = \frac{-G_{\text{BB}}}{[(\frac{1}{2}\nu)^2 - G_{\text{BB}}^2]^{1/2} + \frac{1}{2}\nu} \quad (7)$$

In Eq. (7) G_{BB} is the Breit-Bethe matrix element in frequency units, and ν is the measured $n \ ^1F_3 - n \ ^3F_3$ splitting. The results are given in Table IV. Mixing coefficients for $n=6, 7, 10$, and 11 are also included in the table based on the $^1F_3 - ^3F_3$ splittings reported in Refs. 4 and 5.

APPENDIX

We have carried out numerical experiments to test the appropriateness of the (3, 5, 7) fitting model, Eq. (1), in the case of the helium $n \ ^1P_1 - n \ ^1D_2$ series. Such expansions have been used by several authors.^{4, 5, 8, 12, 23, 24} We used Seaton's Ritz-

TABLE IV. Singlet-triplet mixing coefficients Ω calculated from Eq. (7). Results of other workers are shown. Statistical errors in our results for Ω are much smaller than the likely errors in the Breit-Bethe approximation.

State	Ω	Other results ^a
$6 \ ^3F_3$	0.604 ^b	0.395
$7 \ ^3F_3$	0.574 ^b	0.363
$8 \ ^3F_3$	0.554 ^c	0.343
$9 \ ^3F_3$	0.540 ^c	0.331
$10 \ ^3F_3$	0.551 ^d	0.322
$11 \ ^3F_3$	0.515 ^d	

^a Van den Eynde *et al.*, Ref. 9.

^b MacAdam and Wing, Ref. 5.

^c Present work.

^d Calculated from measurements by Wing *et al.*, Ref. 4.

series coefficients¹⁸ to calculate splittings in this series for $n=3$ to 32, which were used as primary data. We then used the linear least-squares routine to fit subsets of the data using a (3, 4, 5, 6, 7, 8) model, i.e., one containing inverse third through eighth powers of n , as well as several other models, in particular (3, 4, 5) and (3, 5, 7). Equal weighting was used. The resulting parameters clearly showed the expected alternation of magnitudes; those for odd powers were large, those for even powers small. The contributions to the total splitting from each term evaluated at $n=3, 10$, and 18 are given in Table V. From the table we see that while the three most important exponents for low n are 2, 5, and 7, for high n the most important are 3, 4, and 5. Therefore a set of real data in which the accurate measurements are predominantly at high n may well be better fitted by a (3, 4, 5) model than by a (3, 5, 7) model. A data set containing two or three low- n values, however, will be better fitted by the (3, 5, 7) model. This is the case that obtains in the analysis of the $n \ ^1P_1 - n \ ^1D_2$ splittings in Sec. IV A.

Since the pseudodata of these numerical experiments were derived from known Ritz-series coefficients, it should be possible to come full circle using expressions like Eqs. (4)–(6) in the text and to reobtain the coefficients. The extent to which we fail is a measure of the error introduced by selecting only certain exponents, e.g., 3, 5, and 7, in the least-squares fitting. We can also assess the error introduced by fitting only a subset of the data, $n=3, 4, 5, \dots, 32$. We find that the errors attributable to data selection are negligible, at least comparing the results using $n=3-32$ with those using $n=3-10$ and 16–18. The errors attributable to selection of only certain exponents in the model are more important. In particular, the Ritz-coefficient difference ΔC_2 obtained from a (3, 5, 7) model using $n=3-10$ and 16–18 data is likely to be in error by -0.13% . The $|\Delta C_2|$ error from a (3, 4, 5, 6, 7, 8) model using the same data would be only a few parts per mil-

TABLE V. Contributions (MHz) to the $n^1P_1-n^1D_2$ intervals for various n 's and models. Data $n=3-10$ and $16-18$ from Seaton quantum defects, Ref. 18.

Model	n	$A^{(3)}/n^3$	$A^{(4)}/n^4$	$A^{(5)}/n^5$	$A^{(6)}/n^6$	$A^{(7)}/n^7$	$A^{(8)}/n^8$	Total of columns 3-8	Exact ^a
(3, 4, 5, 6, 7, 8)	3	3 464 105.9	-17 481.1	-272 509.2	2150.8	-47 933.9	224.4	3 128 556.9	3 128 557.0
	10	93 530.9	-141.6	-662.2	1.6	-10.5	0.0	92 718.2	92 718.2
	18	16 037.5	-13.5	-35.0	0.0	-0.2	0.0	15 988.8	15 988.9
(3, 5, 7)	3	3 459 773.3		-290 542.4		-40 673.0		3 128 557.9	3 128 557.0
	10	93 413.9		-706.0		-8.9		92 699.0	92 718.2
	18	16 017.5		-37.4		-0.1		15 980.0	15 988.9

^a Calculated directly from Seaton's quantum defects, Ref. 18.

lion. The error in $|\Delta C_3|$ would be +6.4% in a (3, 5, 7) fit compared with -0.2% in a (3, 4, 5, 6, 7, 8) fit. The errors in a (3, 4, 5) model would be -0.9% and +54% for $|\Delta C_2|$ and $|\Delta C_3|$, respectively. The uncertainties quoted in Table III for the Ritz-coefficient differences ΔC_2 and ΔC_3 do not include these model-dependent errors but reflect only

the much smaller statistical uncertainties in the (3, 5, 7) model used. In order to fit *real* data with more than three parameters to reduce these model-dependent errors, we need more experimental data of high absolute accuracy, particularly for $n \leq 10$.

† Work supported in part by the National Science Foundation.

¹W. H. Wing, D. L. Mader, and W. E. Lamb, Jr., *Bull. Am. Phys. Soc.* **16**, 531 (1971).

²W. E. Lamb, Jr., D. L. Mader, and W. H. Wing, in *Fundamental and Applied Laser Physics, Proceedings of the Esfahan Symposium*, edited by M. S. Feld, A. Javan, and N. A. Kurnit (Wiley, New York, 1973), pp. 523-538.

³W. H. Wing and W. E. Lamb, Jr., *Phys. Rev. Lett.* **28**, 265 (1972).

⁴W. H. Wing, K. R. Lea, and W. E. Lamb, Jr., in *Atomic Physics 3*, edited by S. J. Smith and G. K. Walters (Plenum, New York, 1973) pp. 119-141.

⁵K. B. MacAdam and W. H. Wing, *Phys. Rev. A* **12**, 1464 (1975).

⁶A. Javan, in Ref. 2, p. 307.

⁷T. N. Chang and R. T. Poe, *Phys. Rev. A* **10**, 1981 (1974).

⁸T. N. Chang and R. T. Poe, *Phys. Rev. A* (to be published).

⁹R. K. van den Eynde, G. Wiebes, and Th. Niemeyer, *Physica (Utr.)* **59**, 401 (1972).

¹⁰R. M. Parish and R. W. Mires, *Phys. Rev. A* **4**, 2145 (1971).

¹¹T. A. Miller, R. S. Freund, F. Tsai, T. J. Cook, and B. R. Zegarski, *Phys. Rev. A* **9**, 2974 (1974); T. A. Miller, R. S. Freund, and B. R. Zegarski, *ibid.* **11**, 753 (1975).

¹²J. Derouard, R. Jost, M. Lombardi, T. A. Miller,

and R. S. Freund, *Phys. Rev. A*, to be published.

¹³H. J. Beyer and K. J. Kollath, *J. Phys. B* **8**, L326 (1975).

¹⁴H. J. Beyer and K. J. Kollath (private communication).

¹⁵An approximate line-shape theory that treats the passage of the excited atoms out of the detector field of view has been given by S. L. Kaufman, W. E. Lamb, Jr., K. R. Lea, and M. Leventhal, *Phys. Rev. A* **4**, 2128 (1971).

¹⁶Scaled as n^3 from $n=8$ results given by A. H. Gabriel and D. W. O. Heddle, *Proc. R. Soc. A* **258**, 124 (1960).

¹⁷W. E. Lamb, Jr., and R. C. Retherford, *Phys. Rev.* **79**, 549 (1950), Appendix II. The result we quote is not altered by the fact that these authors treated a static perturbation, while the present case involves an oscillatory field.

¹⁸M. J. Seaton, *Proc. Phys. Soc. Lond.* **88**, 815 (1966).

¹⁹The least-squares routine is adapted from CURFIT in P. R. Bevington, *Data Reduction and Error Analysis for the Physical Sciences* (McGraw-Hill, New York, 1969).

²⁰W. C. Hamilton, *Statistics in Physical Science* (Ronald, New York, 1964).

²¹W. C. Martin, *J. Phys. Chem. Ref. Data* **2**, 257 (1973).

²²W. C. Martin, *J. Res. Natl. Bur. Stand. (U.S.) A* **64**, 19 (1960).

²³T. N. Chang, *J. Phys. B* **7**, L108 (1973).

²⁴C. Fabre, M. Gross, and S. Haroche, *Opt. Commun.* **13**, 393 (1975).